Electronic Supplementary Material (ESI) for Physical Chemistry Chemical Physics.

Supporting information

Edge engineering on layered WS_2 toward the electrocatalytic reduction of CO_2: a first principles study

Likai Tong [a], Bo Zhang [a], Yu Zhang [a], Zhijian Peng [b] and Xiuli Fu [a, *]

[a] *State Key Laboratory of Information Photonics and Optical Communications, and School of Integrated Circuits, Beijing University of Posts and Telecommunications, Beijing 100876, P. R. China*

[b] *School of Science, China University of Geosciences, Beijing 100083, P.R. China*

*Corresponding author:

Xiuli Fu (xiulifu@bupt.edu.cn).

Table S1 DFT calculated energy, zero-point energy, entropy, and Gibbs free energy of the gas phase molecules considered in this work

Molecule	E/eV	ZPE/eV	-TS/eV	G/eV
CO_2	-22.95	0.31	-0.66	-23.30
CO	-14.77	0.13	-0.61	-15.25
H_2O	-14.22	0.58	-0.67	-14.31
H_2	-6.77	0.27	-0.40	-6.90

Here, the Gibbs free energy change of intermediates are given by **Equations S1 and S2:**[1]

$$\Delta G\left(COOH*\right) = G\left(COOH*\right) - G* - G\left(CO_2\right) - 1/2G\left(H_2\right) + \Delta G\left(PH\right) \quad \text{(S1)}$$

$$\Delta G\left(CO*\right) = G\left(CO*\right) + G\left(H_2O\right) - G* - G\left(CO_2\right) - G\left(H_2\right) + \Delta G\left(PH\right) \quad \text{(S2)}$$

The solvation correction is given by **Equations S3 and S4:**

$$\Delta G_{corr}\left(COOH*\right) = \Delta G\left(COOH*\right) + \Delta E_{sol}\left(COOH\right) \quad \text{(S3)}$$

$$\Delta G_{corr}\left(CO*\right) = \Delta G\left(CO*\right) + \Delta E_{sol}\left(CO\right) \quad \text{(S4)}$$

The solvation correction to adsorbate energy could be applied to both COOH* (-0.25 eV) and CO* (-0.1 eV).[2]

Table S2 DFT calculated cohesive energy of different models

Models	△G(COOH*)/eV	△G(CO*)/eV
WS_2-3W	-0.75	-1.15
WS_2-4W	-0.70	-1.19

We compared the semi-infinite strip model with 3 W atoms (WS_2-3W) in a direction with the semi-infinite strip model with 4 W atoms (WS_2-4W) in a direction. The calculated values of △G(COOH*) and △G(CO*) show that the WS_2-3W model is similar to the previous studies in literature.[3, 4] In the WS_2-3W model, the distance between the adsorption intermediate of adjacent lattices is 9.54 Å, which can avoid the contact between the adjacent lattices.

Table S3 DFT calculated cohesive energy of different models

Models	cohesive energy (eV/atom)
WS_2	5.56
WS_2-1Zn	5.39
WS_2-2Zn	5.17
WS_2-3Zn	4.96
WS_2-1Fe	5.49
WS_2-2Fe	5.41
WS_2-3Fe	5.33
WS_2-1Co	5.52
WS_2-2Co	5.46
WS_2-3Co	5.39
WS_2-1Ni	5.52
WS_2-2Ni	5.47
WS_2-3Ni	5.41

Table S4 DFT calculated adsorption energy of the intermediates COOH and CO onto different models

Models	Concentration	Adsorption site	$\Delta E_{ads}(COOH*)$/eV	$\Delta E_{ads}(CO*)$/eV
WS_2	0	W	-4.17	-2.45
WS_2-1Zn-1	1/3	W	-3.79	-2.49
WS_2-1Zn-2	1/3	Zn	-1.78	-0.22
WS_2-2Zn-1	2/3	W	-3.79	-1.80
WS_2-2Zn-2	2/3	Zn	-1.91	-0.23
WS_2-3Zn-2	1	Zn	-1.89	-0.39
WS_2-1Fe-1	1/3	W	-3.98	-2.81
WS_2-1Fe-2	1/3	Fe	-2.59	-2.01
WS_2-2Fe-1	2/3	W	-4.11	-2.22
WS_2-2Fe-2	2/3	Fe	-2.66	-2.24
WS_2-3Fe-2	1	Fe	-2.50	-1.78
WS_2-1Co-1	1/3	W	-3.99	-2.14
WS_2-1Co-2	1/3	Co	-2.58	-1.76
WS_2-2Co-1	2/3	W	-4.02	-2.04
WS_2-2Co-2	2/3	Co	-2.66	-1.92
WS_2-3Co-2	1	Co	-2.48	-2.03
WS_2-1Ni-1	1/3	W	-4.06	-2.26
WS_2-1Ni-2	1/3	Ni	-2.35	-0.97
WS_2-2Ni-1	2/3	W	-3.99	-2.10
WS_2-2Ni-2	2/3	Ni	-2.24	-0.93
WS_2-3Ni-2	1	Ni	-2.32	-1.22

Table S5 The calculated Gibbs free energy change at 298.15 K for the adsorption of the intermediates COOH and CO onto different models

Models	Concentration	Adsorption site	△G(COOH*)/eV	△G(CO*)/eV	△G(H*)/eV
WS_2	0	W	-0.75	-1.15	-0.47
WS_2-1Zn-1	1/3	W	-0.38	-1.19	-0.43
WS_2-1Zn-2	1/3	Zn	1.62	1.05	1.62
WS_2-2Zn-1	2/3	W	-0.37	-0.51	0.17
WS_2-2Zn-2	2/3	Zn	1.50	1.06	0.18
WS_2-3Zn-2	1	Zn	1.52	0.88	1.75
WS_2-1Fe-1	1/3	W	-0.56	-1.50	-0.49
WS_2-1Fe-2	1/3	Fe	0.82	-0.69	0.84
WS_2-2Fe-1	2/3	W	-0.68	-0.93	-0.12
WS_2-2Fe-2	2/3	Fe	0.75	-0.91	-0.10
WS_2-3Fe-2	1	Fe	0.91	-0.46	0.93
WS_2-1Co-1	1/3	W	-0.58	-0.83	-0.43
WS_2-1Co-2	1/3	Co	0.83	-0.43	0.77
WS_2-2Co-1	2/3	W	-0.60	-0.75	-0.02
WS_2-2Co-2	2/3	Co	0.75	-0.60	0.67
WS_2-3Co-2	1	Co	0.93	-0.71	0.87
WS_2-1Ni-1	1/3	W	-0.65	-0.95	-0.65
WS_2-1Ni-2	1/3	Ni	1.06	0.34	1.10
WS_2-2Ni-1	2/3	W	-0.57	-0.81	0.04
WS_2-2Ni-2	2/3	Ni	1.18	0.38	1.14
WS_2-3Ni-2	1	Ni	1.09	0.09	1.10

Table S6 Bond lengths in the considered models

Models	Concentration	Adsorption site	COOH*/Å			CO*/Å
			d_{M-C}	d_{M-O1}	d_{M-O2}	d_{W-C}
WS_2	0	W	2.05	2.24	3.30	2.00
WS_2-1Zn-1	1/3	W	2.04	2.19	3.31	1.92
WS_2-1Zn-2	1/3	Zn	2.04	2.94	2.83	2.11
WS_2-2Zn-1	2/3	W	2.07	2.22	3.32	2.03
WS_2-2Zn-2	2/3	Zn	2.03	2.91	2.83	2.09
WS_2-3Zn-2	1	Zn	2.04	2.91	2.84	2.08
WS_2-1Fe-1	1/3	W	2.03	2.18	3.30	1.91
WS_2-1Fe-2	1/3	Fe	1.91	2.65	2.89	1.74
WS_2-2Fe-1	2/3	W	2.05	2.24	3.30	2.01
WS_2-2Fe-2	2/3	Fe	1.93	2.70	2.89	1.75
WS_2-3Fe-2	1	Fe	1.96	2.71	2.91	1.77
WS_2-1Co-1	1/3	W	2.03	2.16	3.30	2.01
WS_2-1Co-2	1/3	Co	1.92	2.81	2.78	1.75
WS_2-2Co-1	2/3	W	2.06	2.23	3.30	2.03
WS_2-2Co-2	2/3	Co	1.93	2.82	2.78	1.75
WS_2-3Co-2	1	Co	1.92	2.74	2.83	1.74
WS_2-1Ni-1	1/3	W	2.04	2.18	3.31	2.00
WS_2-1Ni-2	1/3	Ni	1.95	2.83	2.78	1.81
WS_2-2Ni-1	2/3	W	2.06	2.22	3.30	2.01
WS_2-2Ni-2	2/3	Ni	1.96	2.84	2.78	1.82
WS_2-3Ni-2	1	Ni	1.95	2.82	2.76	1.81

Table S7 Solvent corrected $\Delta G_{corr}(COOH*)$ values (in eV) at different PH in the considered models

Models	PH														
	0	1	2	3	4	5	6	7	8	9	10	11	12	13	14
WS_2	-1.00	-0.94	-0.88	-0.82	-0.76	-0.71	-0.65	-0.59	-0.53	-0.47	-0.41	-0.35	-0.29	-0.23	-0.17
WS_2-1Zn-1	-0.63	-0.57	-0.51	-0.45	-0.39	-0.33	-0.27	-0.22	-0.16	-0.10	-0.04	0.02	0.08	0.14	0.20
WS_2-1Zn-2	1.37	1.43	1.49	1.55	1.61	1.67	1.73	1.79	1.85	1.90	1.96	2.02	2.08	2.14	2.20
WS_2-2Zn-1	-0.62	-0.56	-0.50	-0.44	-0.38	-0.32	-0.26	-0.20	-0.14	-0.08	-0.02	0.04	0.09	0.15	0.21
WS_2-2Zn-2	1.25	1.31	1.37	1.43	1.49	1.55	1.60	1.66	1.72	1.78	1.84	1.90	1.96	2.02	2.08
WS_2-3Zn-2	1.27	1.33	1.39	1.45	1.51	1.56	1.62	1.68	1.74	1.80	1.86	1.92	1.98	2.04	2.10
WS_2-1Fe-1	-0.81	-0.75	-0.69	-0.63	-0.58	-0.52	-0.46	-0.40	-0.34	-0.28	-0.22	-0.16	-0.10	-0.04	0.02
WS_2-1Fe-2	0.57	0.63	0.69	0.75	0.81	0.87	0.92	0.98	1.04	1.10	1.16	1.22	1.28	1.34	1.40
WS_2-2Fe-1	-0.93	-0.88	-0.82	-0.76	-0.70	-0.64	-0.58	-0.52	-0.46	-0.40	-0.34	-0.28	-0.22	-0.16	-0.11
WS_2-2Fe-2	0.50	0.56	0.62	0.68	0.74	0.80	0.86	0.92	0.97	1.03	1.09	1.15	1.21	1.27	1.33
WS_2-3Fe-2	0.66	0.72	0.78	0.84	0.90	0.96	1.02	1.08	1.14	1.20	1.25	1.31	1.37	1.43	1.49
WS_2-1Co-1	-0.83	-0.77	-0.71	-0.65	-0.59	-0.53	-0.47	-0.41	-0.35	-0.29	-0.24	-0.18	-0.12	-0.06	0.00
WS_2-1Co-2	0.58	0.64	0.70	0.76	0.82	0.88	0.94	1.00	1.06	1.12	1.18	1.23	1.29	1.35	1.41
WS_2-2Co-1	-0.85	-0.79	-0.73	-0.67	-0.61	-0.55	-0.49	-0.43	-0.37	-0.31	-0.26	-0.20	-0.14	-0.08	-0.02
WS_2-2Co-2	0.50	0.56	0.62	0.67	0.73	0.79	0.85	0.91	0.97	1.03	1.09	1.15	1.21	1.27	1.33
WS_2-3Co-2	0.68	0.74	0.79	0.85	0.91	0.97	1.03	1.09	1.15	1.21	1.27	1.33	1.39	1.45	1.51
WS_2-1Ni-1	-0.90	-0.84	-0.78	-0.72	-0.66	-0.60	-0.54	-0.48	-0.42	-0.36	-0.31	-0.25	-0.19	-0.13	-0.07
WS_2-1Ni-2	0.81	0.87	0.93	0.99	1.05	1.10	1.16	1.22	1.28	1.34	1.40	1.46	1.52	1.58	1.64
WS_2-2Ni-1	-0.82	-0.76	-0.70	-0.64	-0.58	-0.52	-0.46	-0.40	-0.34	-0.28	-0.23	-0.17	-0.11	-0.05	0.01
WS_2-2Ni-2	0.93	0.99	1.04	1.10	1.16	1.22	1.28	1.34	1.40	1.46	1.52	1.58	1.64	1.70	1.76
WS_2-3Ni-2	0.84	0.90	0.96	1.02	1.08	1.14	1.20	1.26	1.32	1.38	1.44	1.49	1.55	1.61	1.67

Table S8 Solvent corrected $^{\Delta G_{corr}(CO*)}$ values (in eV) at different PH in the considered models

Models	PH														
	0	1	2	3	4	5	6	7	8	9	10	11	12	13	14
WS_2	-1.25	-1.19	-1.13	-1.07	-1.02	-0.96	-0.90	-0.84	-0.78	-0.72	-0.66	-0.60	-0.54	-0.48	-0.42
WS_2-1Zn-1	-1.29	-1.23	-1.17	-1.11	-1.05	-0.99	-0.93	-0.87	-0.81	-0.76	-0.70	-0.64	-0.58	-0.52	-0.46
WS_2-1Zn-2	0.95	1.01	1.07	1.13	1.19	1.25	1.31	1.37	1.42	1.48	1.54	1.60	1.66	1.72	1.78
WS_2-2Zn-1	-0.61	-0.55	-0.49	-0.44	-0.38	-0.32	-0.26	-0.20	-0.14	-0.08	-0.02	0.04	0.10	0.16	0.22
WS_2-2Zn-2	0.96	1.02	1.08	1.14	1.20	1.26	1.32	1.37	1.43	1.49	1.55	1.61	1.67	1.73	1.79
WS_2-3Zn-2	0.78	0.84	0.90	0.96	1.02	1.08	1.14	1.20	1.26	1.32	1.38	1.43	1.49	1.55	1.61
WS_2-1Fe-1	-1.60	-1.54	-1.48	-1.43	-1.37	-1.31	-1.25	-1.19	-1.13	-1.07	-1.01	-0.95	-0.89	-0.83	-0.77
WS_2-1Fe-2	-0.79	-0.73	-0.67	-0.61	-0.55	-0.49	-0.43	-0.37	-0.31	-0.25	-0.20	-0.14	-0.08	-0.02	0.04
WS_2-2Fe-1	-1.03	-0.97	-0.91	-0.85	-0.79	-0.73	-0.67	-0.61	-0.55	-0.49	-0.43	-0.37	-0.32	-0.26	-0.20
WS_2-2Fe-2	-1.01	-0.95	-0.89	-0.83	-0.77	-0.71	-0.66	-0.60	-0.54	-0.48	-0.42	-0.36	-0.30	-0.24	-0.18
WS_2-3Fe-2	-0.56	-0.51	-0.45	-0.39	-0.33	-0.27	-0.21	-0.15	-0.09	-0.03	0.03	0.09	0.15	0.21	0.26
WS_2-1Co-1	-0.93	-0.88	-0.82	-0.76	-0.70	-0.64	-0.58	-0.52	-0.46	-0.40	-0.34	-0.28	-0.22	-0.16	-0.10
WS_2-1Co-2	-0.53	-0.48	-0.42	-0.36	-0.30	-0.24	-0.18	-0.12	-0.06	0.00	0.06	0.12	0.18	0.24	0.29
WS_2-2Co-1	-0.85	-0.79	-0.73	-0.67	-0.61	-0.55	-0.49	-0.44	-0.38	-0.32	-0.26	-0.20	-0.14	-0.08	-0.02
WS_2-2Co-2	-0.70	-0.64	-0.58	-0.52	-0.46	-0.40	-0.34	-0.28	-0.23	-0.17	-0.11	-0.05	0.01	0.07	0.13
WS_2-3Co-2	-0.81	-0.75	-0.69	-0.63	-0.57	-0.51	-0.45	-0.39	-0.33	-0.27	-0.21	-0.15	-0.09	-0.03	0.02
WS_2-1Ni-1	-1.05	-0.99	-0.94	-0.88	-0.82	-0.76	-0.70	-0.64	-0.58	-0.52	-0.46	-0.40	-0.34	-0.28	-0.22
WS_2-1Ni-2	0.24	0.30	0.36	0.42	0.47	0.53	0.59	0.65	0.71	0.77	0.83	0.89	0.95	1.01	1.07
WS_2-2Ni-1	-0.91	-0.85	-0.79	-0.73	-0.67	-0.61	-0.55	-0.49	-0.43	-0.37	-0.31	-0.25	-0.20	-0.14	-0.08
WS_2-2Ni-2	0.28	0.34	0.40	0.46	0.52	0.58	0.64	0.70	0.76	0.82	0.88	0.93	0.99	1.05	1.11
WS_2-3Ni-2	0.00	0.06	0.12	0.18	0.24	0.29	0.35	0.41	0.47	0.53	0.59	0.65	0.71	0.77	0.83

Table S9 Solvent corrected U_L values (in V) at different PH in the considered models

Models	PH														
	0	1	2	3	4	5	6	7	8	9	10	11	12	13	14
WS_2	-1.25	-1.19	-1.13	-1.07	-1.02	-0.96	-0.90	-0.84	-0.78	-0.72	-0.66	-0.60	-0.54	-0.48	-0.42
WS_2-1Zn-1	-1.29	-1.23	-1.17	-1.11	-1.05	-0.99	-0.93	-0.87	-0.81	-0.76	-0.70	-0.64	-0.58	-0.52	-0.46
WS_2-1Zn-2	-1.37	-1.43	-1.49	-1.55	-1.61	-1.67	-1.73	-1.79	-1.85	-1.90	-1.96	-2.02	-2.08	-2.14	-2.20
WS_2-2Zn-1	-0.61	-0.55	-0.49	-0.44	-0.38	-0.32	-0.26	-0.20	-0.14	-0.08	-0.02	-0.04	-0.09	-0.15	-0.21
WS_2-2Zn-2	-1.25	-1.31	-1.37	-1.43	-1.49	-1.55	-1.60	-1.66	-1.72	-1.78	-1.84	-1.90	-1.96	-2.02	-2.08
WS_2-3Zn-2	-1.27	-1.33	-1.39	-1.45	-1.51	-1.56	-1.62	-1.68	-1.74	-1.80	-1.86	-1.92	-1.98	-2.04	-2.10
WS_2-1Fe-1	-1.60	-1.54	-1.48	-1.43	-1.37	-1.31	-1.25	-1.19	-1.13	-1.07	-1.01	-0.95	-0.89	-0.83	-0.77
WS_2-1Fe-2	-0.79	-0.73	-0.69	-0.75	-0.81	-0.87	-0.92	-0.98	-1.04	-1.10	-1.16	-1.22	-1.28	-1.34	-1.40
WS_2-2Fe-1	-1.03	-0.97	-0.91	-0.85	-0.79	-0.73	-0.67	-0.61	-0.55	-0.49	-0.43	-0.37	-0.32	-0.26	-0.20
WS_2-2Fe-2	-1.01	-0.95	-0.89	-0.83	-0.77	-0.80	-0.86	-0.92	-0.97	-1.03	-1.09	-1.15	-1.21	-1.27	-1.33
WS_2-3Fe-2	-0.66	-0.72	-0.78	-0.84	-0.90	-0.96	-1.02	-1.08	-1.14	-1.20	-1.25	-1.31	-1.37	-1.43	-1.49
WS_2-1Co-1	-0.93	-0.88	-0.82	-0.76	-0.70	-0.64	-0.58	-0.52	-0.46	-0.40	-0.34	-0.28	-0.22	-0.16	-0.10
WS_2-1Co-2	-0.58	-0.64	-0.70	-0.76	-0.82	-0.88	-0.94	-1.00	-1.06	-1.12	-1.18	-1.23	-1.29	-1.35	-1.41
WS_2-2Co-1	-0.85	-0.79	-0.73	-0.67	-0.61	-0.55	-0.49	-0.44	-0.38	-0.32	-0.26	-0.20	-0.14	-0.08	-0.02
WS_2-2Co-2	-0.70	-0.64	-0.62	-0.67	-0.73	-0.79	-0.85	-0.91	-0.97	-1.03	-1.09	-1.15	-1.21	-1.27	-1.33
WS_2-3Co-2	-0.81	-0.75	-0.79	-0.85	-0.91	-0.97	-1.03	-1.09	-1.15	-1.21	-1.27	-1.33	-1.39	-1.45	-1.51
WS_2-1Ni-1	-1.05	-0.99	-0.94	-0.88	-0.82	-0.76	-0.70	-0.64	-0.58	-0.52	-0.46	-0.40	-0.34	-0.28	-0.22
WS_2-1Ni-2	-0.81	-0.87	-0.93	-0.99	-1.05	-1.10	-1.16	-1.22	-1.28	-1.34	-1.40	-1.46	-1.52	-1.58	-1.64
WS_2-2Ni-1	-0.91	-0.85	-0.79	-0.73	-0.67	-0.61	-0.55	-0.49	-0.43	-0.37	-0.31	-0.25	-0.20	-0.14	-0.08
WS_2-2Ni-2	-0.93	-0.99	-1.04	-1.10	-1.16	-1.22	-1.28	-1.34	-1.40	-1.46	-1.52	-1.58	-1.64	-1.70	-1.76
WS_2-3Ni-2	-0.84	-0.90	-0.96	-1.02	-1.08	-1.14	-1.20	-1.26	-1.32	-1.38	-1.44	-1.49	-1.55	-1.61	-1.67

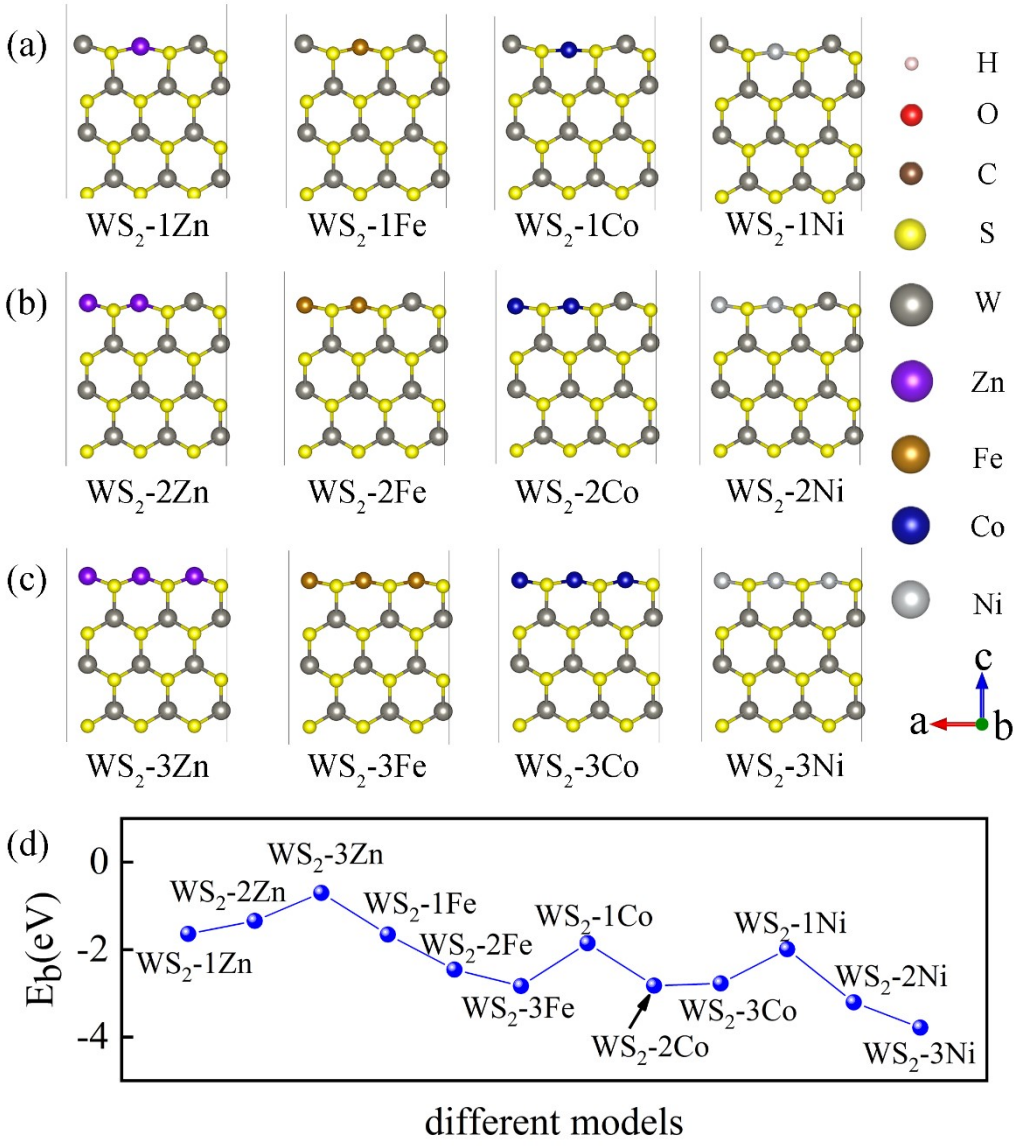

Figure S1 Optimized stable structures of (a) WS_2-1TM models, (b) WS_2-2TM models and (c) WS_2-3TM models. (d) Binding energy of WS_2-xTM. The binding energy (E_b) is calculated by the following formula: $E_b=E(WS_2\text{-xTM})-\mu TM-E(WS_2\text{-}V_W)$, where $E(WS_2\text{-xTM})$ and $E(WS_2\text{-}V_W)$ are the energy of WS_2-xTM model and the energy of WS_2 with W vacancy, respectively, and μTM is the energy of each TM atom in its bulk phase.

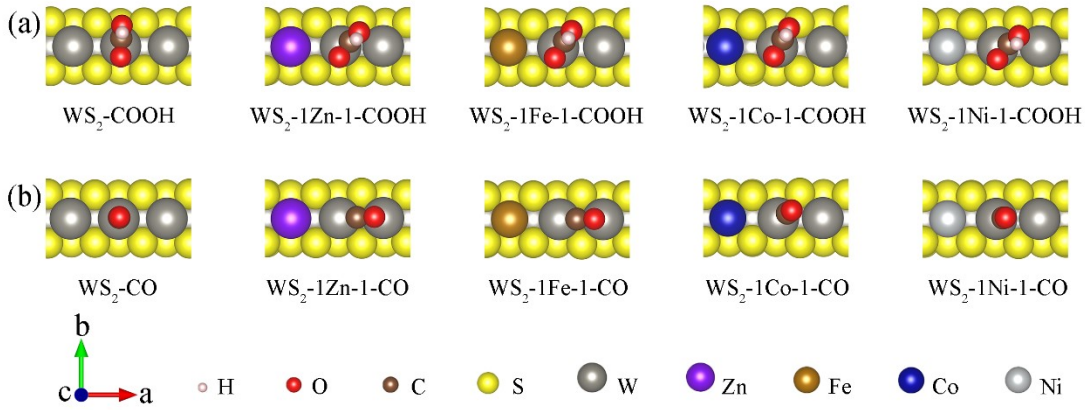

Figure S2 Stable structures of WS_2 and WS_2-1TM-1 models absorbed with reaction intermediates (a) COOH* and (b) CO*, respectively

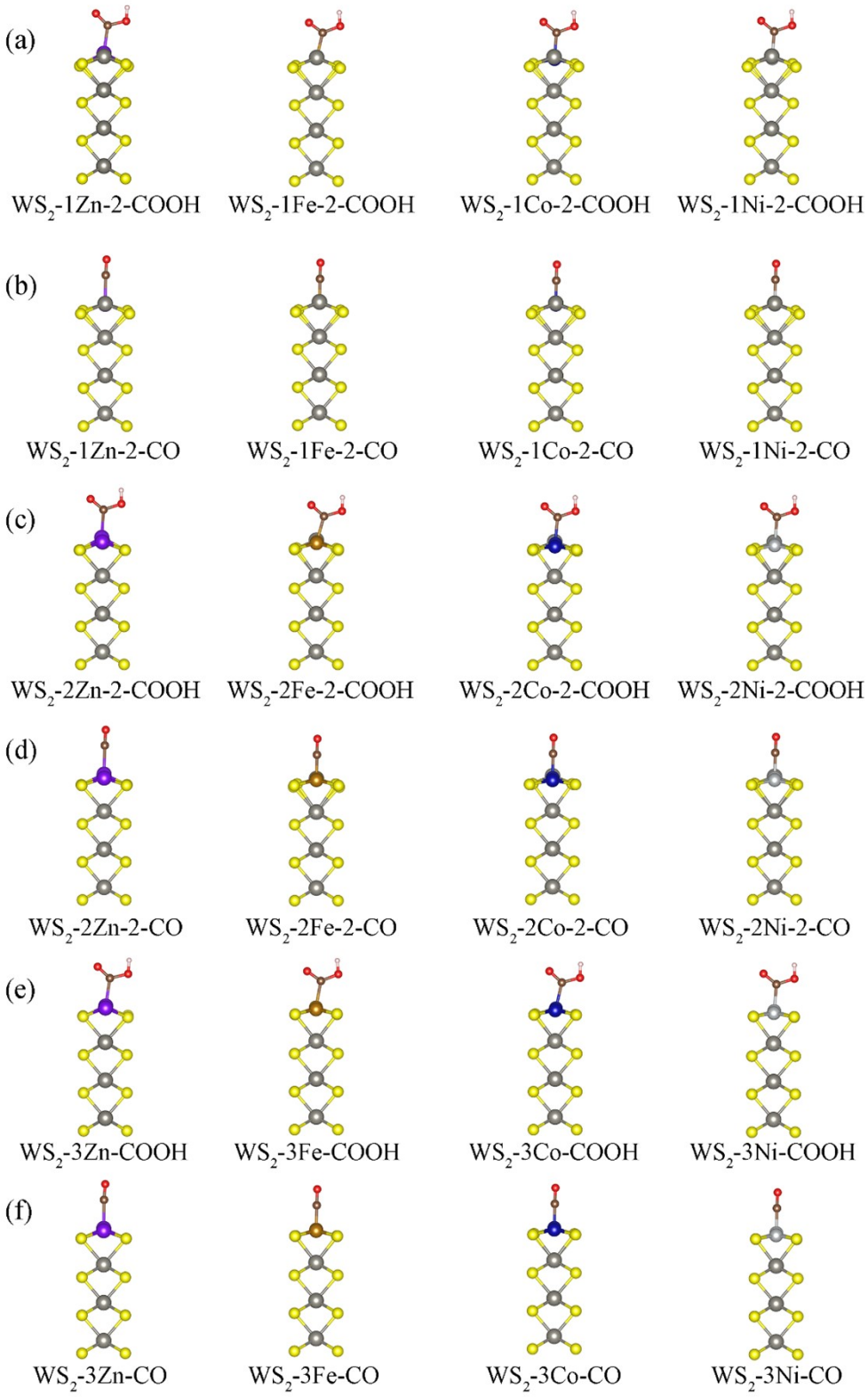

Figure S3 Stable structures of WS_2-1TM-2 models absorbed with reaction intermediates (a) COOH* and (b) CO*, respectively; stable structures of WS_2-2TM-2 models absorbed with reaction intermediates (c) COOH* and (d) CO*, respectively; and stable structures of WS_2-3TM models absorbed with reaction intermediates (e) COOH* and (f) CO*, respectively

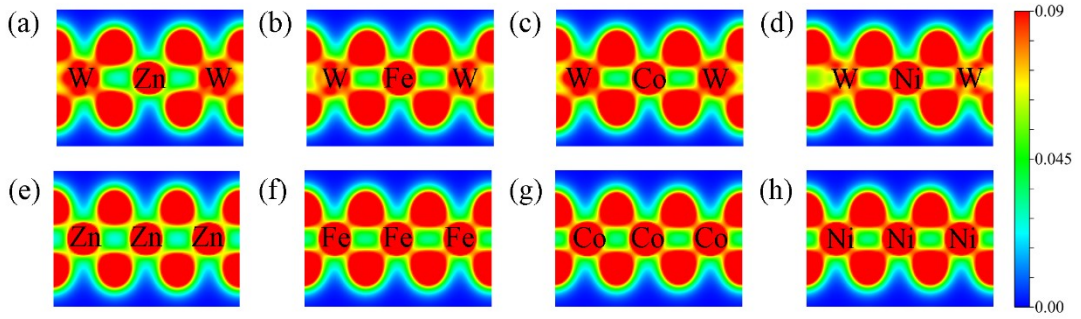

Figure S4 Charge density for (a) WS_2-1Zn, (b) WS_2-1Fe, (c) WS_2-1Co, (d) WS_2-1Ni, (e) WS_2-3Zn, (f) WS_2-3Fe, (g) WS_2-3Co and (h) WS_2-3Ni models.

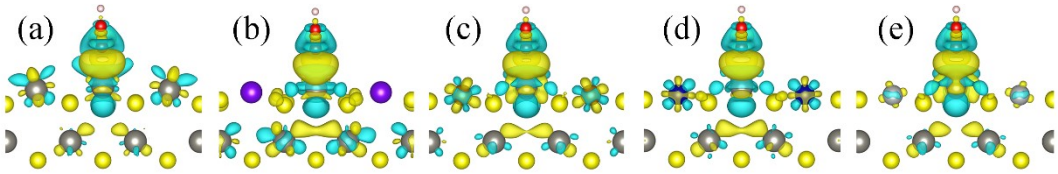

Figure S5 The side view of charge density difference for the adsorption of COOH* on (a) bare WS_2, (b) WS_2-2Zn-1, (c) WS_2-2Fe-1, (d) WS_2-2Co-1 and (e) WS_2-2Ni-1 models. The charge accumulation/depletion is shown in yellow/cyan with the isosurface of 0.002 e/Å^3 • c. The gray, blue, yellow, brown, red and white balls in the ball-and-stick models represent the W, Zn, S, C, O and H atoms, respectively.

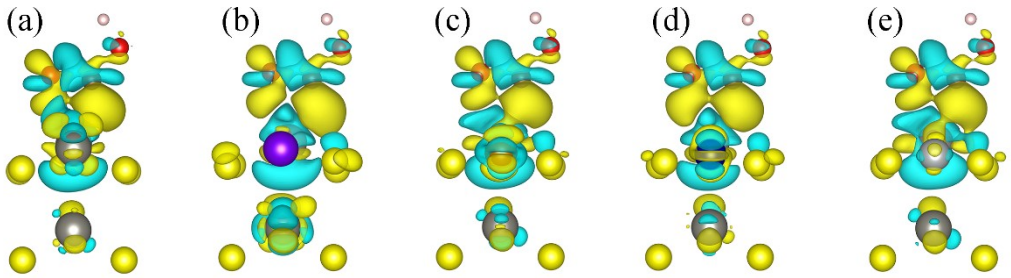

Figure S6 The main view of charge density difference for the adsorption of COOH* on (a) bare WS_2, (b) WS_2-2Zn-1, (c) WS_2-2Fe-1, (d) WS_2-2Co-1 and (e) WS_2-2Ni-1 models. The charge accumulation/depletion is shown in yellow/cyan with the isosurface of 0.002 e/Å^3 • c. The gray, blue, yellow, brown, red and white balls in the ball-and-stick models represent the W, Zn, S, C, O and H atoms, respectively.

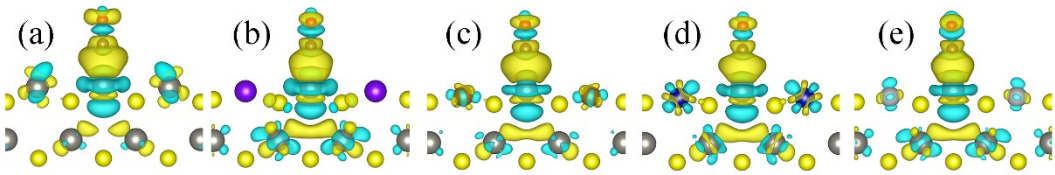

Figure S7 The side view of charge density difference for the adsorption of CO* on (a) bare WS_2, (b) WS_2-2Zn-1, (c) WS_2-2Fe-1, (d) WS_2-2Co-1 and (e) WS_2-2Ni-1 models. The charge accumulation/depletion is shown in yellow/cyan with the isosurface of 0.002 e/Å^3 • c. The gray, blue, yellow, brown, red and white balls in the ball-and-stick models represent the W, Zn, S, C, O and H atoms, respectively.

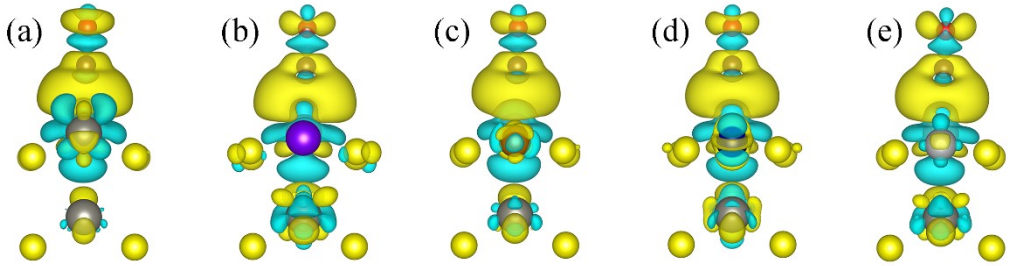

Figure S8 The main view of charge density difference for the adsorption of CO* on (a) bare WS_2, (b) WS_2-2Zn-1, (c) WS_2-2Fe-1, (d) WS_2-2Co-1 and (e) WS_2-2Ni-1 models. The charge accumulation/depletion is shown in yellow/cyan with the isosurface of 0.002 e/Å^3 • c. The gray, blue, yellow, brown, red and white balls in the ball-and-stick models represent the W, Zn, S, C, O and H atoms, respectively.

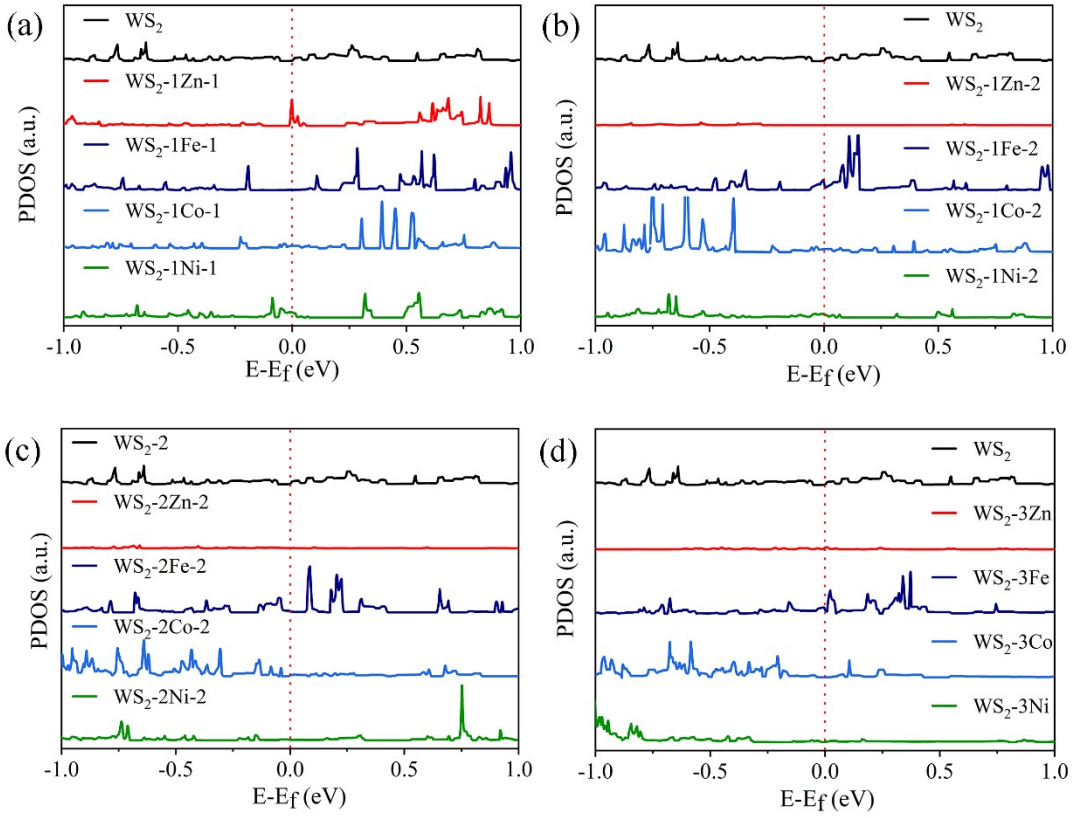

Figure S9 Projected state density of d-orbit of adsorption site in (a) WS_2-1TM-1, (b) WS_2-1TM-2, (c) WS_2-2TM-2, and (d) WS_2-3TM models.

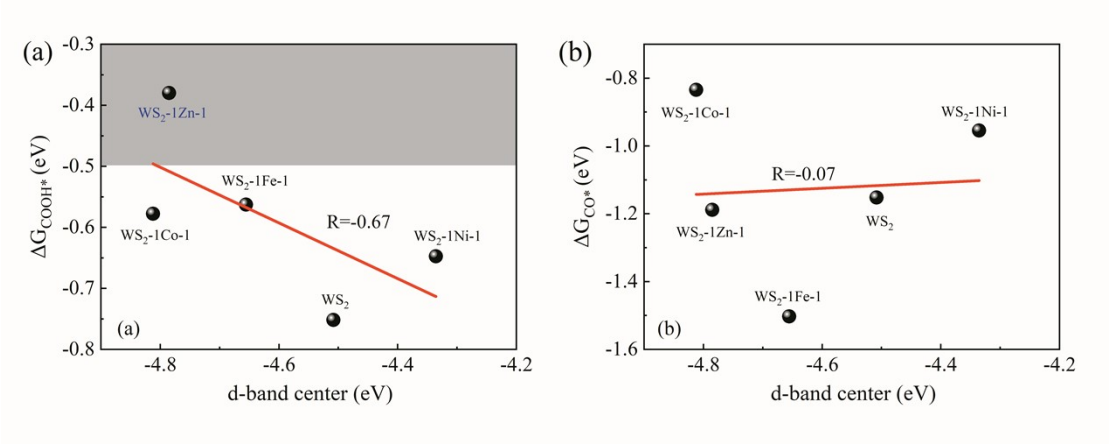

Figure S10 Relationship between the Gibbs free energy change and d-band centers of W sites in WS_2-1TM models in the case of absorption intermediate(a) COOH* and (b) CO*, respectively. The R shows the correlation between Gibbs free energy and d-band centers. The gray region indicates the models with better electrocatalytic performance ($-0.5 < \Delta G < 0.5$ eV).

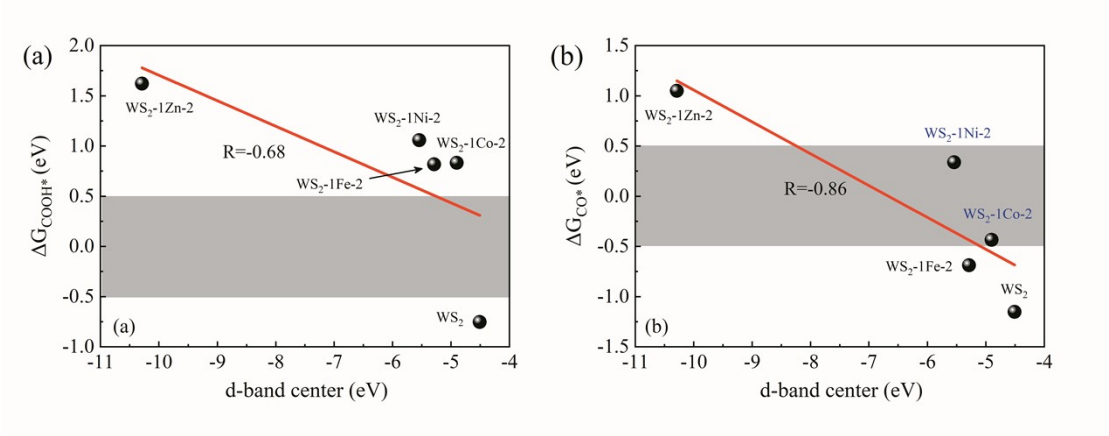

Figure S11 Relationship between the Gibbs free energy change and d-band centers of TM sites in WS_2-1TM models in the case of absorption intermediate(a) COOH* and (b) CO*, respectively. The R shows the correlation between Gibbs free energy and d-band centers. The gray region indicates the models with better electrocatalytic performance (-0.5＜ΔG＜0.5 eV).

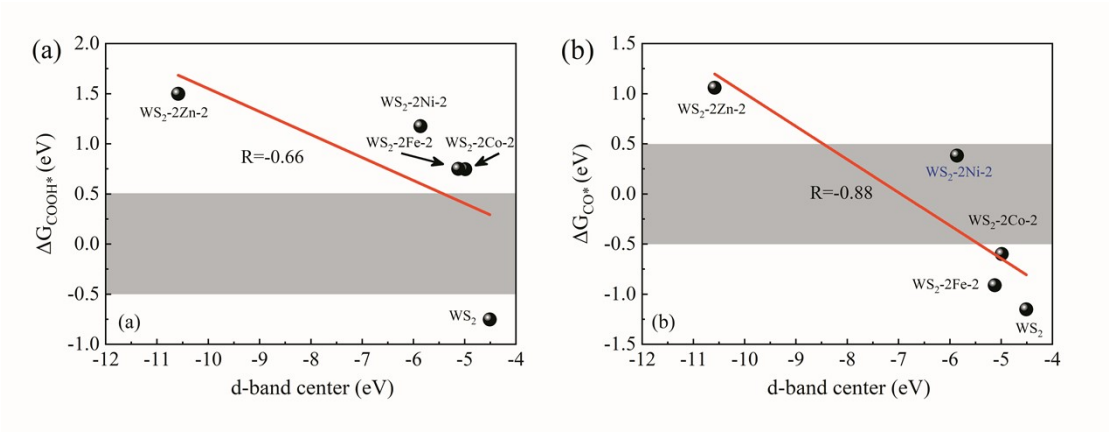

Figure S12 Relationship between the Gibbs free energy change and d-band centers of TM sites in WS_2-2TM models in the case of absorption intermediate(a) COOH* and (b) CO*, respectively. The R shows the correlation between Gibbs free energy and d-band centers. The gray region indicates the models with better electrocatalytic performance (-0.5＜ΔG＜0.5 eV).

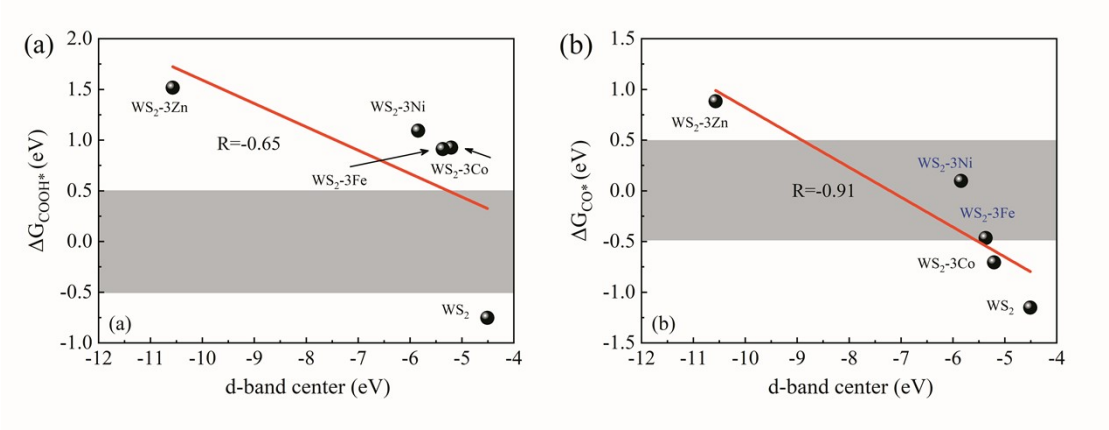

Figure S13 Relationship between the Gibbs free energy change and d-band centers of TM sites in WS_2-3TM models in the case of absorption intermediate(a) COOH* and (b) CO*, respectively. The R shows the correlation between Gibbs free energy and d-band centers. The gray region indicates the models with better electrocatalytic performance (-0.5＜ΔG＜0.5 eV).

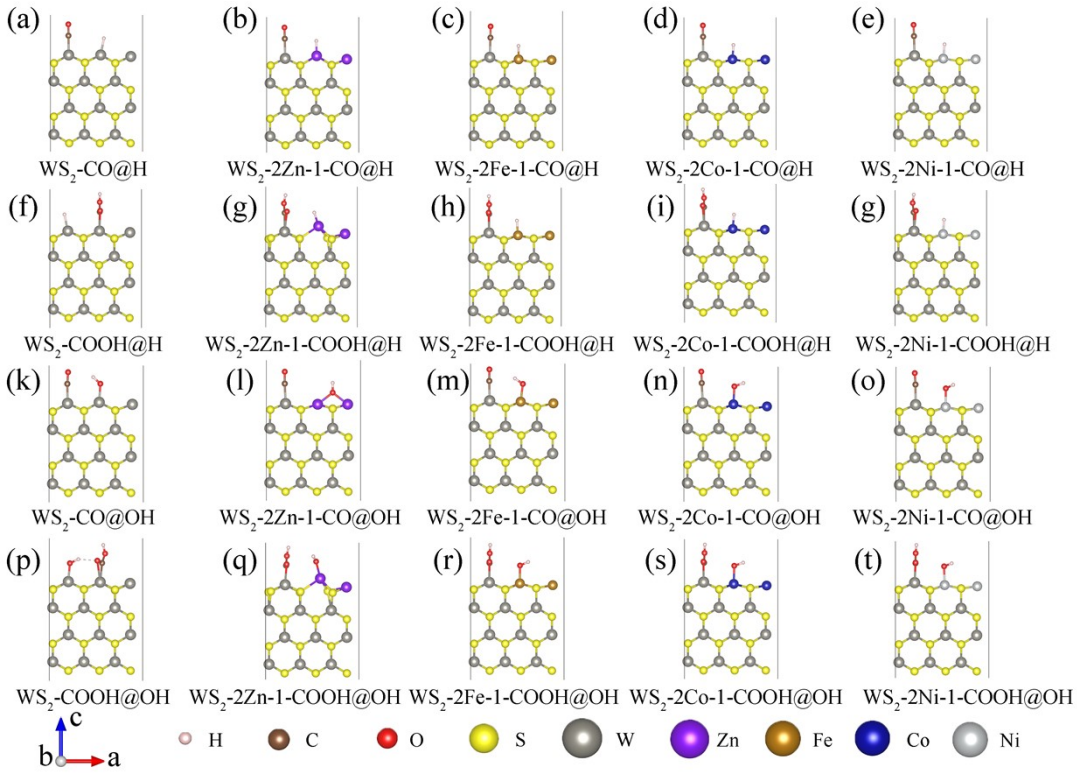

Figure S14 Stable structures of (a) WS_2, (b) WS_2-2Zn-1, (c) WS_2-2Fe-1, (d) WS_2-2Co-1 and (e) WS_2-2Ni-1 models absorbed with reaction intermediates CO* and H*, respectively. Stable structures of (f) WS_2, (g) WS_2-2Zn-1, (h) WS_2-2Fe-1, (i) WS_2-2Co-1 and (j) WS_2-2Ni-1 models absorbed with reaction intermediates COOH* and H*, respectively. Stable structures of (k) WS_2,

(l) WS_2-2Zn-1, (m) WS_2-2Fe-1, (n) WS_2-2Co-1 and (o) WS_2-2Ni-1 models absorbed with reaction intermediates CO* and OH*, respectively. Stable structures of (p) WS_2, (q) WS_2-2Zn-1, (r) WS_2-2Fe-1, (s) WS_2-2Co-1 and (t) WS_2-2Ni-1 models absorbed with reaction intermediates COOH* and OH*, respectively.

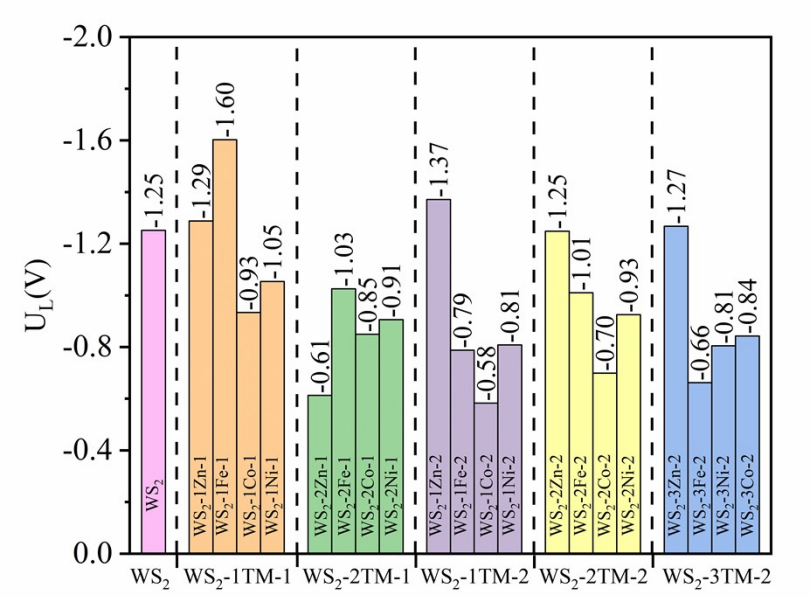

Figure S15 The calculated values of limiting potential (U_L) after solvation modification for the CO_2RR to CO on different models at PH=0.

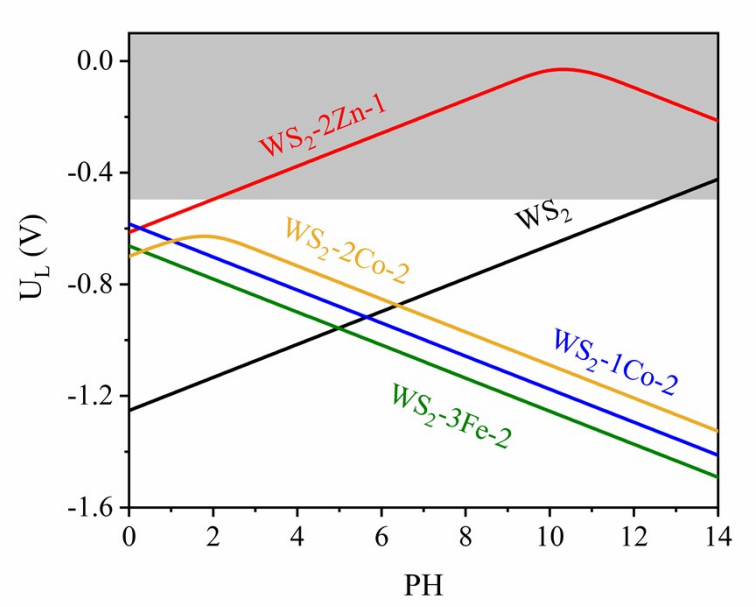

Figure S16 The calculated values of limiting potential (U_L) after solvation modification for the CO_2RR to CO on WS_2, WS_2-1Co-2, WS_2-2Co-2, WS_2-2Zn-1 and WS_2-3Fe-2 models at different PH.

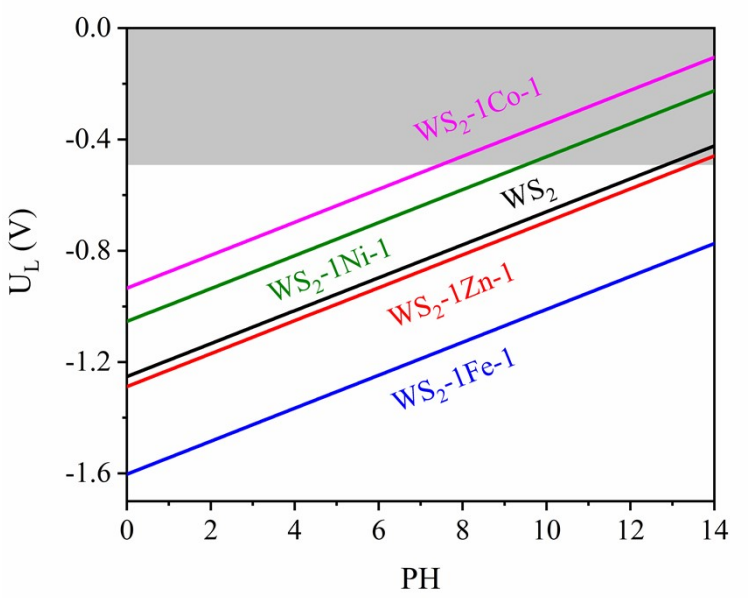

Figure S17 The calculated values of limiting potential (U_L) after solvation modification for the CO_2RR to CO on WS_2-1TM-1 models at different PH.

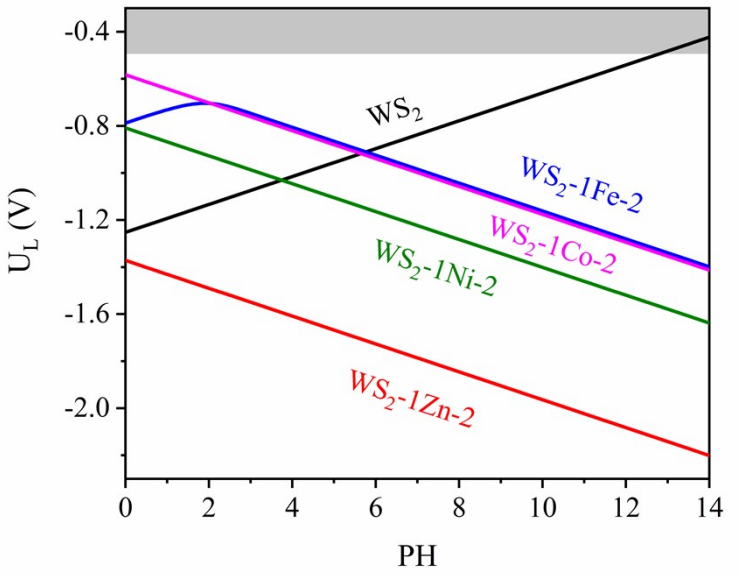

Figure S18 The calculated values of limiting potential (U_L) after solvation modification for the CO_2RR to CO on WS_2-1TM-2 models at different PH.

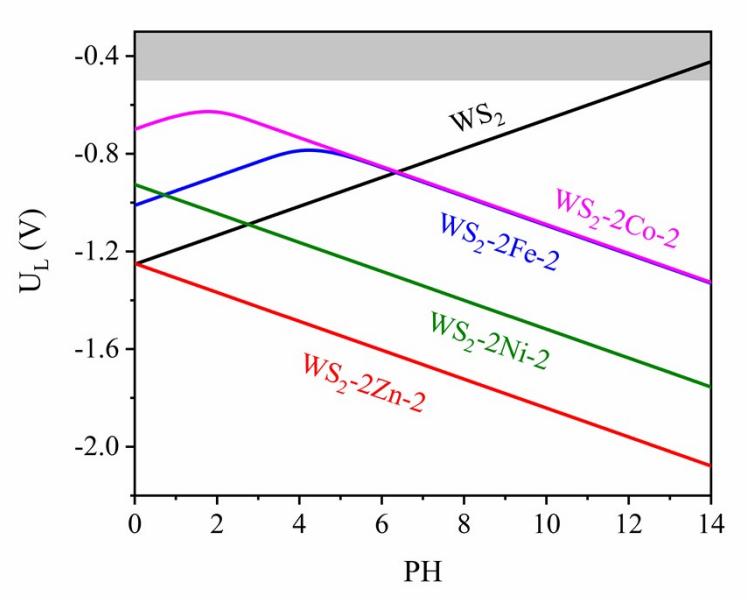

Figure S19 The calculated values of limiting potential (U_L) after solvation modification for the CO_2RR to CO on WS_2-2TM-2 models at different PH.

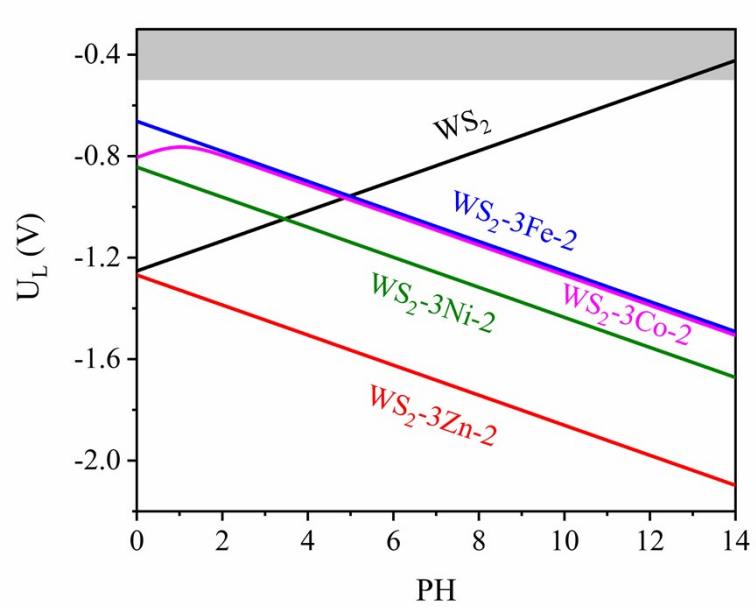

Figure S20 The calculated values of limiting potential (U_L) after solvation modification for the CO_2RR to CO on $WS_2$3TM-2 models at different PH.

Reference

1. P. Prslja and N. López, *ACS Catalysis*, 2021, **11**, 88-94.
2. A. A. Peterson and J. K. Nørskov, *The Journal of Physical Chemistry Letters*, 2012, **3**, 251-258.
3. M. Asadi, K. Kim, C. Liu, A. V. Ad Depalli, P. Abbasi, P. Yasaei, P. Phillips, A. Behranginia, J. M. Cerrato and R. Haasch, *Science*, 2016, **353**, 467.
4. P. Abbasi, M. Asadi, C. Liu, S. Sharifi-Asl, B. Sayahpour, A. Behranginia, P. Zapol, R. Shahbazian-Yassar, L. A. Curtiss and A. Salehi-Khojin, *Acs Nano*, 2017, **11**, 453-460.